coatings

MDPI

Article

The Effect of Magnesium Chloride on the Macroscopic and MI-Croscopic Properties of Phosphate Cement-Based Materials

Yubing Du [1,2,3,*], Zhaoyu Wang [1], Peiwei Gao [2], Jianming Yang [1], Shucong Zhen [1], Hui Wang [4,*] and Tao Du [5]

1 College of Civil Engineering, Yancheng Institute of Technology, Yancheng 224051, China; zywang@ycit.cn (Z.W.); yjm_kk@ycit.cn (J.Y.); zhenshucong@ycit.cn (S.Z.)
2 Department of Civil and Airport Engineering, College of Civilaviation (College of Flight), Nanjing University of Aeronautics and Astronautics, Nanjing 210016, China; gpw1963@nuaa.edu.cn
3 Jiangsu Collaborative Innovation Center for Ecological Building Materials and Environmental Protection, Yancheng 224051, China
4 School of Civil and Environmental Engineering, Ningbo University, Ningbo 315000, China
5 School of Mechanics and Civil Engineering, China University of Mining and Technology, Xuzhou 221116, China; dutao@cumt.edu.cn
* Correspondence: duyubing@ycit.cn (Y.D.); huiwang123@aliyun.com (H.W.)

Abstract: Phosphate cement-based materials are fast-hardening cement materials, which have been applied to the rapid repair of concrete structures. However, the excessive setting rate could lead to initial cracks in the cement-based matrix. Therefore, a proper retarder is required to reduce the setting rate, thus improving the strength of structures. In this study, a magnesium chloride retarder was selected, and its influence on the setting time, slump flow, and the mechanical strengths (flexural strength, compressive strength, and bond strength) of phosphate cement paste curing for 3 h~28 d was investigated. Scanning electron microscopy, X-ray diffraction, and thermal analysis were used to analyze the mechanism of the properties of phosphate cement paste. Results showed that the setting time increased exponentially with the mass ratio of magnesium chloride by the total mass of magnesium oxide. Meanwhile, the slump flow increased linearly with the increasing dosage of magnesium chloride, and the drying shrinkage rate exhibited a quadratic function with the curing age. The addition of magnesium chloride decreased the mechanical strengths of phosphate cement paste at earlier curing age (lower than 3 d) and effectively improved the mechanical strengths at a later curing age (equal to or higher than 3 d). Moreover, magnesium chloride could also decrease the drying shrinkage rate. It can be obtained from the microcosmic researching results that magnesium chloride can inhibit the hydration of phosphate cement and reduce cracks induced by drying shrinkage at later curing age (higher than 3 d).

Keywords: phosphate cement; magnesium chloride; setting time; mechanical strengths; scanning electron microscope; X-ray diffraction; thermal analysis

check for updates

Citation: Du, Y.; Wang, Z.; Gao, P.; Yang, J.; Zhen, S.; Wang, H.; Du, T. The Effect of Magnesium Chloride on the Macroscopic and MI-Croscopic Properties of Phosphate Cement-Based Materials. *Coatings* **2022**, *12*, 370. https://doi.org/10.3390/coatings12030370

Academic Editor: Paolo Castaldo

Received: 10 February 2022
Accepted: 7 March 2022
Published: 10 March 2022

Publisher's Note: MDPI stays neutral with regard to jurisdictional claims in published maps and institutional affiliations.

Copyright: © 2022 by the authors. Licensee MDPI, Basel, Switzerland. This article is an open access article distributed under the terms and conditions of the Creative Commons Attribution (CC BY) license (https://creativecommons.org/licenses/by/4.0/).

1. Introduction

In recent years, the damage of cement concrete building structures is frequently reported. For some critical structures, such as bridges and roads, it is always needed to recover their function.

For timely operation and use [1], the materials mainly used to repair bridge decks include early strength Portland cement concrete, fast hardening sulfate cement repair materials, emulsified asphalt concrete, polymer-modified cement or polymer cemented repair materials, etc. [2–5]. However, using Portland cement as a repair material has the drawbacks of low early strength, high maintenance requirements, volume stability, and poor bonding [6,7]. Fast-hardening sulfate cement, which can develop its strength in a short time, has been broadly used as a repair material for road repair. Research has shown that it can be opened to traffic after paving within 6 h [8]. Besides, it also offers high early

strength, strong frost resistance, good impermeability, and corrosion resistance. However, this repair material is prone to micro expansion in humid environments. This material may generate large hydration heat and thermal cracks in the early curing stage during hydration [9,10]. Since cracks exist, the inner reinforcement is prone to corrosion, which may cause its strength reduction at a later stage [11]. Therefore, fast-hardening cement with better performance is needed as a substitute.

Magnesium phosphate cement repairing material was manufactured by mixing the neutralization of over-burned magnesium oxide and phosphate with acid and alkali at room temperature [12,13]. This type of cement was first invented by Brookhaven National Laboratory and Argonne National Laboratory in the United States [14,15]. The mechanical properties, the microscopic properties, and the durability of magnesium phosphate cement-based materials have been reported by several scholars [16–18]. Prior research pointed out that magnesium phosphate cement repair material has the advantages of rapid setting and hardening, high strength, low shrinkage cracking, and wear resistance. However, its setting and hardening speeds are difficult to control, hindering its large-scale production and application [19,20]. Therefore, the application of retarder in magnesium phosphate cement is very important.

Retarders, such as borax, boric acid, triethanolamine, are commonly used in phosphate cement. It has been proven that borax and boric acid can delay the setting of cement, reduce the hydration heat, and prevent early cracking [21,22]. Moreover, the addition of borax and boric acid can improve the mechanical strength at a later curing age [23,24]. However, the retarding efficiencies of borax and boric acid are low. A large amount of borax and boric acid needs to be added to the cement to achieve an effective retarding effect, which may further significantly increase the manufacturing cost of magnesium phosphate cement-based materials. The triethanolamine possessed an excellent retarding effect [25]. Nevertheless, this kind of retarder may reduce the mechanical strength. To this end, a newly developed retarder was proposed.

In this study, a kind of self-developed retarder (magnesium chloride mixed with fixed content of borax) was applied in the magnesium phosphate cement paste. The setting time and the mechanical strengths (flexural strength, compressive strength and bond strength) were investigated. Thermogravimetric analysis, X-ray diffraction, and scanning electron microscopy were carried out for investigating the hydration mechanism. This research will promote the application of magnesium phosphate cement in the future.

2. Experimental Section

2.1. Raw Materials

The grinded magnesium oxide produced by Hebei Gaolin Magnesium Salt Chemical Co., Ltd., Gancang, China, was used for the preparation of magnesium phosphate cement. The specific surface area, density, average diameter, melting point, and boiling point of grinded magnesium oxide are 395 m^2/kg, 3.17 g/cm^3, 67.16 μm, 2852 °C, and 3600 °C, respectively. The potassium dihydrogen phosphate applied in this research was manufactured by Guangdong Xilong Chemical Co., Guangzhou, China. The borax, with an average diameter of 53.12 μm, was provided by Dashiqiao Yongtai borax factory, Dashiqiao, China. The purities of magnesium oxide, potassium dihydrogen phosphate, and borax were 91.47%, 98.1%, and 98.5%, respectively. Table 1 shows the main chemical composition of magnesium oxide powder.

Table 1. Main chemical composition of magnesium oxide powder.

Oxide	MgO	SiO_2	Al_2O_3	CaO	Fe_xO_y	TiO_2	Loss on Ignition
Content/%	91.47	3.27	1.13	1.98	1.17	0.03	0.95

2.2. Specimen Preparation

The specimens were manufactured according to the mixing proportion of Table 2 following these steps.

Table 2. Mix proportions of magnesium phosphate cement paste/g.

Types	MgO	Borax	K_2HPO_4	$MgCl_2$	Water	Water-Reducer
$MgCl_2$-0	100	2.5	2	0	15.7	0.31
$MgCl_2$-1	100	2.5	2	1.0	15.8	0.32
$MgCl_2$-2	100	2.5	2	2.0	16	0.32
$MgCl_2$-3	100	2.5	2	3.0	16.1	0.32
$MgCl_2$-4	100	2.5	2	4.0	16.3	0.33

The MgO, borax, and $MgCl_2$ were mixed using a Type JJ-5 cement mixer for 1 min with a stirring speed of 140 ± 5 r/min. After that, water, K_2HPO_4, and water-reducing agent were added to the cement mixer and stirred for another 3 min with a stirring speed of 285 ± 10 r/min. Finally, all fresh RPC was poured into a mold to fabricate the specimens with a size of 40 mm × 40 mm× 160 mm.

2.3. Measurement Methods

2.3.1. The Setting Time Experiment

A circular truncated cone with 60 mm top diameter, 70 mm bottom diameter, and 40 mm height was used to measure the setting time for phosphate cement paste. Cement standard consistency setting time tester (standard favicat tester) cement Vicat was produced by Beijing zhongkejianyi Electronic Technology Co., Ltd., Beijing, China was used to measure the setting time. This experiment was carried out according to GBT1346-2011 [26].

2.3.2. The Experiments of Mechanical Performance

The compressive and flexural strengths of specimens were tested by the YAW-300 microcomputer-controlled full-automatic universal testing machine (Jinan Ruipu Electromechanical Technology Co., Ltd., Jinan, China). The loading speeds of 2.4 kN/s and 0.05 kN/s were selected for determining the compressive and flexural strengths, respectively. The specific test process was conducted according to GB/T 17671-1999 Chinese standard [27]. Figure 1 shows the measurement of flexural and compressive strengths of phosphate cement-based materials.

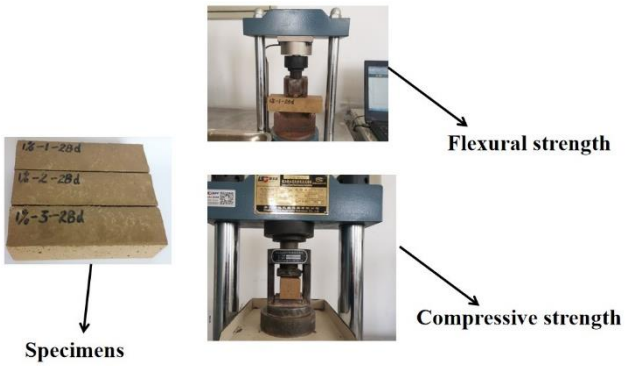

Figure 1. The flexural and compressive strengths of phosphate cement-based materials.

The bond strength of phosphate cement-based materials can be obtained by the following method. The specimens of ordinary Portland cement paste with the water-cement ratio of 0.15% and 0.3% water-reducing agent by cement mass were prepared. The specimens were cured in an environment of 50% relative humidity and temperature of 20 °C for two days and then demolded. The demolded specimens were moved to the standard curing room and cured for 26 days. After curing, all specimens were cut in two

halves, and each half of the specimens was repaired by phosphate cement paste. After hardening, the specimens were cured in the standard environment for 3 h, 1 d, 3 d and 28 d. Finally, the flexural strength of the repaired specimens was determined according to GB/T 17671-1999 Chinese standard. The corresponding flexural strength was the bond strength of phosphate cement paste. Figure 2 illustrates the specimen for the measurement of bond strength.

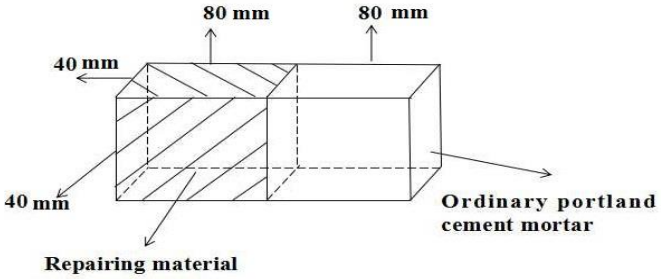

Figure 2. Specimen for the measurement of bond strength.

The drying shrinkage rate was determined by a Swiss SYLVAC high precision digital display 805-8501 ten-thousandth meter provided by Swiss Danqing Technology Co., Ltd., Beijing, China. The Swiss SYLVAC high precision digital display 805-8501 ten-thousandth meter was installed at the axial position of the specimen. The drying shrinkage rate was measured by following these steps.

The specimen's initial length (L_0) was tested after the sample's initial hardening. Then, the value of the length (L_t) of the specimen was read out during the curing time. The drying shrinkage rate (S_d) of concrete can be calculated by Equation (1), and Figure 3 shows the measurement of drying shrinkage rate.

$$S_d = \frac{L_t - L_0}{L_0} \quad (1)$$

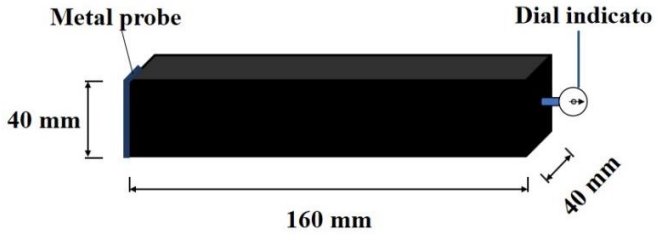

Figure 3. The measurement of drying shrinkage rate.

2.3.3. Experiments of Thermal Analysis and SEM

The following process was carried out for thermal analysis, SEM, and research experiments.

The samples were cured in the standard curing environment for 3 h, 1 day, 3 days, and 28 days. After curing, all samples were immersed in absolute ethanol for 4 days to prevent the hydration of cement. Then, the vacuum drying oven produced by Beijing zhongkejianyi Electronic Technology Co., Ltd., Beijing, China, was used to dry the samples at 60 °C for 4 days. A soybean-sized sample of hardened cement paste was taken from the inner portion of specimens for the following measurements.

The samples were filtrated with a 74 μm sieve in the thermogravimetric test. Meanwhile, some soybean-sized hardened samples coated by gold film were used for measurement via scanning electron microscope (SEM). Nitrogen with a 20 mL/min flow rate was provided as shielding gas. The temperature in the thermogravimetric analyzer ranged from 20 °C to 950 °C. Weighed sample powder was placed in an alumina pan of the confined space of a thermogravimetric analyzer. The experimental process for the thermal analysis curves was referenced from [28–30]. A TGA 4000 thermogravimetric analyzer provided by Perkin Elmer Instrument Co., Ltd., New York, NY, USA and a JSM-6360LV scanning

electron microscope (Japan electron optics laboratory, Tokyo, Japan) were applied in the measurement of SEM images and thermal analysis curves, respectively. The ground powder of specimen was moved to the D8 ADVANCE X-ray diffractometer (Bruker Corp., Tokyo, Japan) for the measurement of the XRD.

3. Results and Discussion

3.1. The Working Performance

The setting time is the one of the main parameters that affects the performance of phosphate cement. Figure 4 shows the initial and final setting time of phosphate cement paste. It can be found from Figure 4 that the initial setting time increased (the increasing rate is 85.2%) with the dosage of magnesium chloride increasing from 0% to 1%. A dramatic increase in the initial setting time was observed with the further addition of dosage from 1% to 2% (the increasing rate was 196.5%). However, with further increases in dosage, this increasing rate decreased. Increasing rates to the initial setting were found for the dosage from 2% to 3% and 3% to 4%. This indicates that the initial setting time increased rapidly with the dosages of magnesium chloride increasing from 0% to 2%. However, the increasing rate of the initial setting time decreased for the dosage from 2% to 4%. Similar results have been found for the final setting time of phosphate cement paste. Moreover, the gap between the initial and final setting time was small at an MgCl content of less than 2%, which could be attributed to the fact that the addition of MgCl could significantly change the pH value of phosphate cement paste. It could inhibit phosphate particles' dissolution and thus retard the early hydration reaction speed of phosphate cement paste. However, when the content of MgCl was less than 2%, the retarding effect of MgCl was insignificant [31,32]. Furthermore, the magnesium chloride can provide magnesium ions. Therefore, with the increase of magnesium chloride, the magnesium ion will increase as well, thus inhibiting the hydration reaction of phosphate cement [33]. At a 2% dosage of magnesium chloride, the optimal retarding efficiency was reached. At this dosage, phosphate cement's initial and final setting times were 33.5 $\pm$ 0.018 min and 56.8 $\pm$ 0.016 min, respectively, which is suitable for construction. As obtained from Figure 4, the error bar value was lower than 0.03, indicating the accuracy of experimental data.

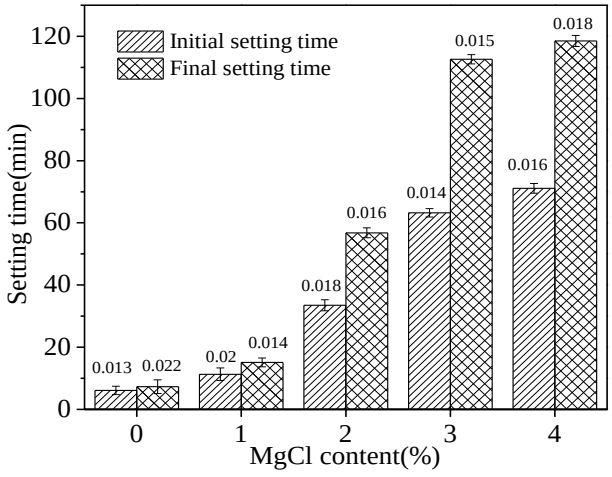

Figure 4. The setting time of cement paste.

The fluidity of phosphate cement paste is the main factor affecting the pouring of fresh phosphate cement paste. Figure 5 shows the slump flow of fresh phosphate cement paste. As illustrated in Figure 5, the slump flow of fresh phosphate cement paste increased in the form of a linear function with the increasing dosage of magnesium chloride. This could be attributed to the fact that the addition of magnesium chloride could delay hydration and condensation of phosphate cement paste, thus decreasing the rate of free water consumption

due to the hydration [18,34]. The relative squared error (R^2) of the fitting function in Figure 5 is 0.96, indicating the rationality and accuracy of the fitting result.

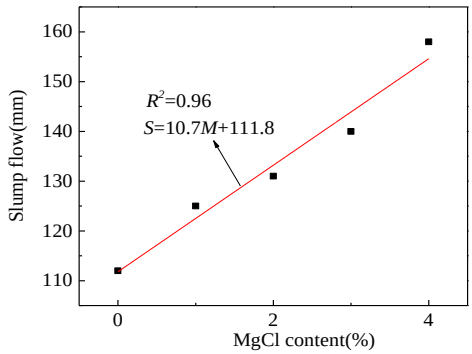

Figure 5. The slump flow of cement paste.

3.2. The Mechanical Performance

As a kind of fast hardening and early strength cement, the phosphate cement paste is prone to cracking due to the huge hydration heat. Figure 6 shows the drying shrinkage rate of specimens, which can be applied to evaluate the crack performance. The corresponding fitting results are illustrated in Table 3. As depicted in Figure 6, the drying shrinkage rate of specimens increased obviously, with the curing age increasing from 0 h to 28 d due to the large amount of hydration heat produced by early hydration of phosphate cement [35,36]. Meanwhile, when the curing age increased from 28 d to 90 d, the drying shrinkage rate reached the peaks and decreased slightly. This could be attributed to the practically completed hydration of phosphate cement at a curing age of 28 d [37]. Moreover, it can be found in Figure 6, the addition of magnesium chloride can result in the reduction of drying shrinkage rate due to the effect of delaying phosphate cement setting and hydration.

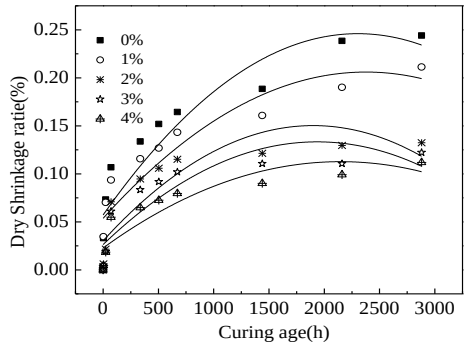

Figure 6. The drying shrinkage rate of specimens.

Table 3. The fitting results of drying shrinkage rate and the curing age (T).

Equation	MgCl Content/%	a	b	c	R^2
$S_d = aT^2 + bT + c$	0	-3.56×10^{-8}	1.64×10^{-4}	0.057	0.83
	1	-2.70×10^{-8}	1.28×10^{-4}	0.054	0.80
	2	-3.32×10^{-8}	1.26×10^{-4}	0.030	0.81
	3	-2.85×10^{-8}	1.10×10^{-4}	0.026	0.80
	4	-1.95×10^{-8}	8.37×10^{-5}	0.023	0.81

Figure 7 shows the mechanical strengths including flexural strength, compressive strength and bond strength of phosphate cement paste. The corresponding increasing rates of mechanical strengths are shown in Figure 7b,d,f respectively. It can be found in Figure 7, the mechanical strengths increased with increasing curing age. When the curing

age was lower than 3 d, the mechanical strengths decreased with the growing dosage of magnesium chloride. However, when the curing age reached 3 d or is higher than 3 d, the addition of magnesium chloride increased the mechanical strengths of phosphate cement paste. All specimens' flexural strength, compressive strength, and bond strength were 2.9 MPa~13.5 MPa, 22.3 MPa~68.6 MPa, and 1.8 MPa~7.56 MPa, confirming that the phosphate cement with retarder possessed high early mechanical strength and bond strength. It can be found from Figure 7 that magnesium chloride can reduce the mechanical strengths of phosphate cement paste at a curing age lower than or equal to 1 d and improve the mechanical strengths at a curing age longer than 3 d. Finally, the error bar values were lower than 0.0071, confirming the precision of the experimental results.

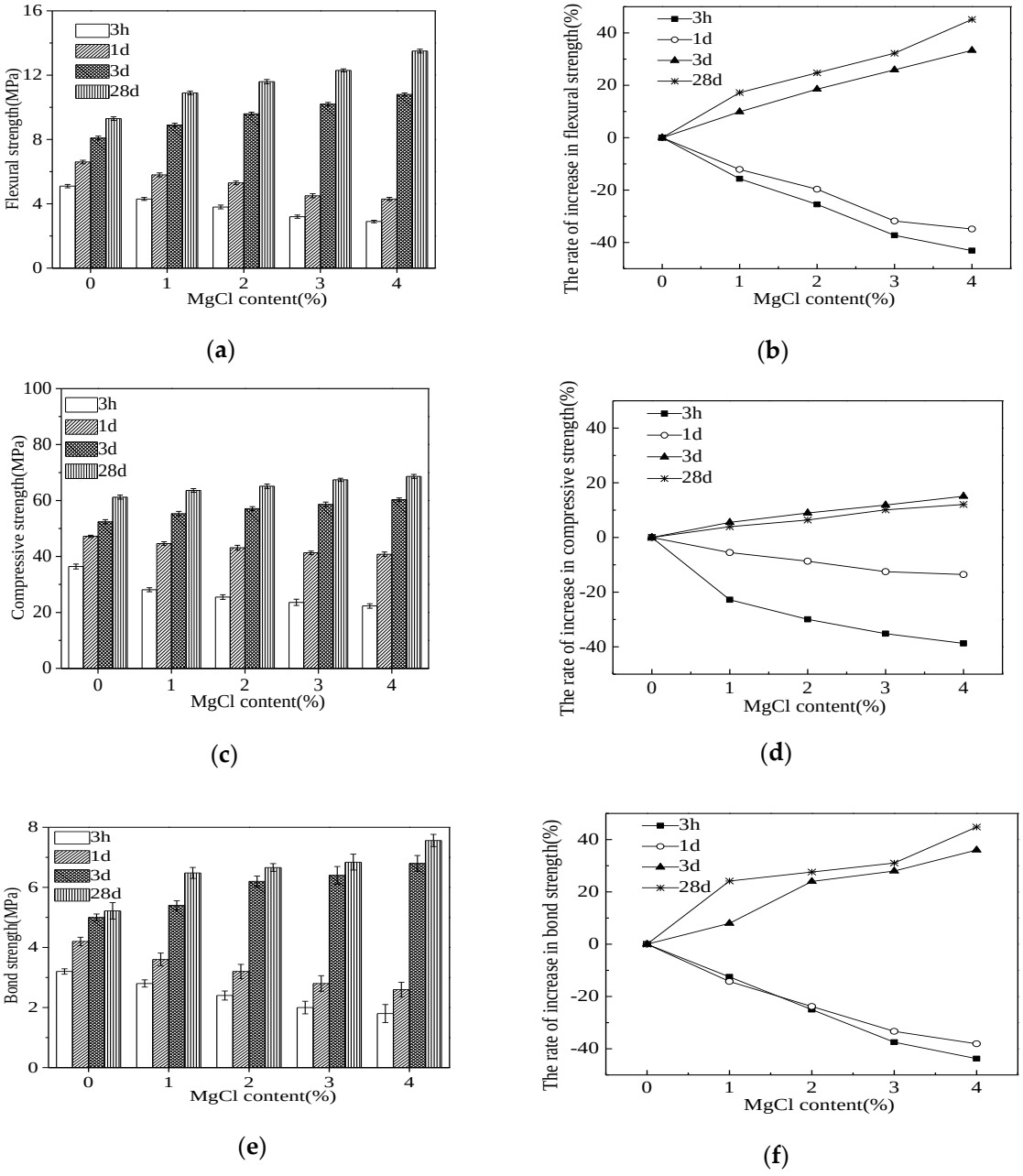

Figure 7. The mechanical strengths and the corresponding increasing rate of cement paste at different curing age. (**a**) Flexural strength, (**b**) The increasing rate of flexural strength by MgCl, (**c**) Compressive strength, (**d**) The increasing rate of flexural strength by MgCl, (**e**) Bond strength, (**f**) The increasing rate of flexural strength by MgCl.

3.3. Microscopic Analysis

In this study, the specimens with 1%, 2%, and 4% were used for microscopic research. Figure 8 shows the thermogravimetric (TG) analysis and differential thermal analysis (DTA) which were applied in characterizing the hydration process of phosphate cement. The testing temperature of the thermal experiment ranged from 20 °C to 950 °C.

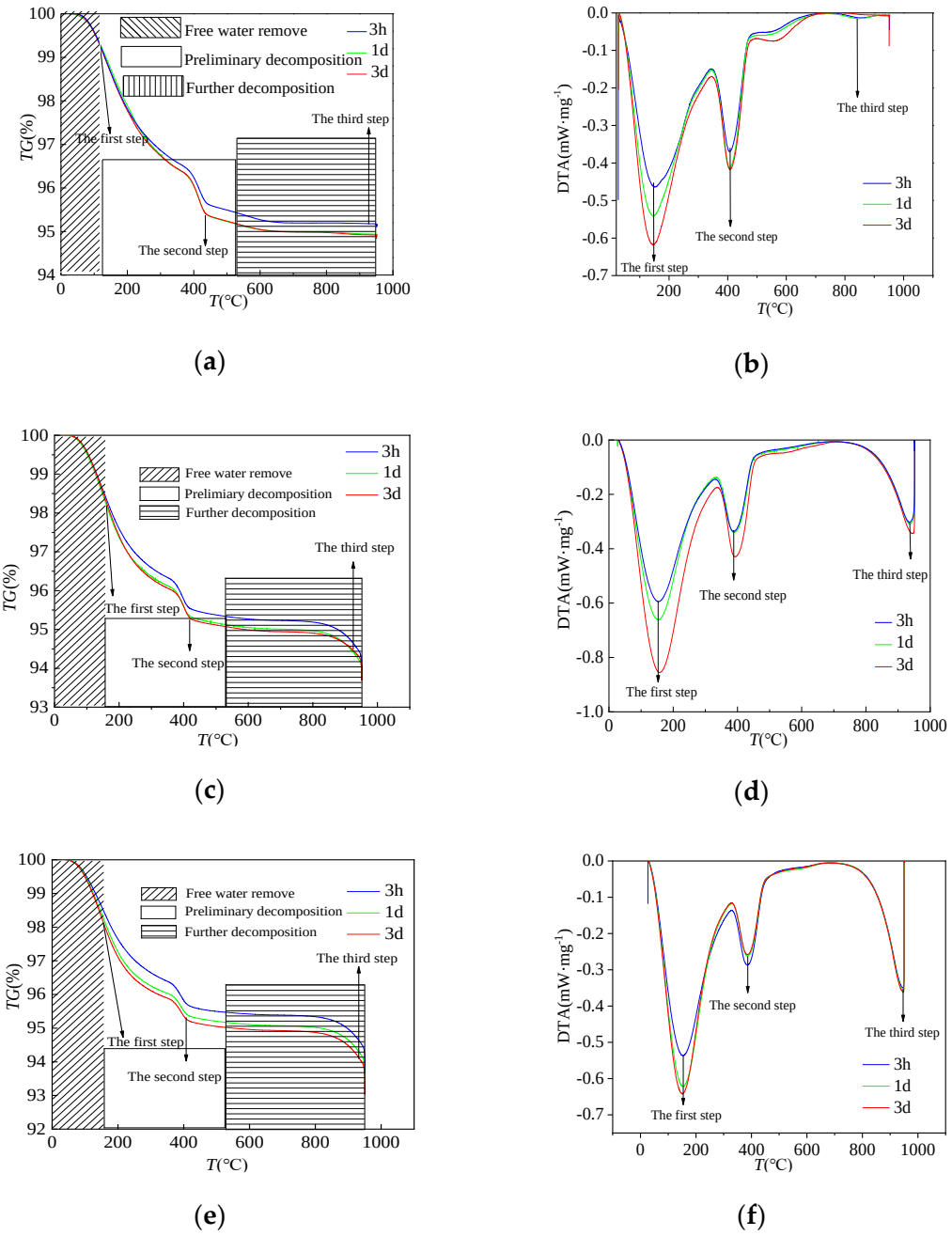

Figure 8. Thermogravimetric analysis curves of specimens. (**a**) TG curves of specimens with 0% MgCl, (**b**) DTA curves of specimens with 0% MgCl, (**c**) TG curves of specimens with 2% MgCl, (**d**) DTA curves of specimens with 2% MgCl, (**e**) TG curves of specimens with 4% MgCl, (**f**) DTA curves of specimens with 4% MgCl.

Figure 8a,c,e demonstrate the TG analysis, which can reflect the weight loss of hydration product under increasing temperature. Additionally, the DTA curves are illustrated in Figure 8b,d,f, which present the peak positions of temperatures. It can be observed from Figure 8 that the TG decreased rapidly as the temperature increased from 20 °C to 424 °C.

However, when the temperature ranged from 424 °C to 950 °C, the TG varied stably with the increasing temperature. The variation of TG and DTA curves can be described as three steps. In the first phase (20 °C~150 °C), the first mutations of TG and DTA occurred, due to the evaporation of free water. Moreover, when the temperature increased to 424 °C, the second mutations of TG and DTA happened due to the early hydration of magnesium phosphate cement (the decomposition of hydrated potassium magnesium phosphate formed by the hydration of magnesium oxide and potassium hydrogen phosphate, in this step some water of crystallization decomposed) [38–41]. The third mutation was at 918 °C, due to the further decomposition of hydrated potassium magnesium phosphate (in this step, more water of crystallization decomposed). Moreover, the addition of magnesium chloride decreased the TG and DTA when the temperature was 424 °C, due to the retarding effect of phosphate cement paste. Furthermore, the magnesium chloride led to increasing the TG and DTA, especially when the temperature was 918 °C. Therefore, the magnesium chloride improved the performance of magnesium phosphate cement paste when the curing age was equal to or higher than 1 d.

Figure 9 shows the X-ray diffraction spectrums of specimens. It can be observed that magnesium oxide (MgO), potassium magnesium phosphate (MKP), and potassium dihydrogen phosphate (KH_2PO_4) existed in the specimens. As depicted in Figure 9, diffraction peaks of the magnesium oxide and potassium dihydrogen phosphate decreased with the increasing curing ages due to the fact that the hydration degree of MgO and KH_2PO_4 was improved by the increasing curing age. Moreover, the addition of magnesium chloride increased the diffraction peaks of the magnesium oxide. The research results can explain the hydration promotion of the increased curing age and the retarding effect of magnesium chloride.

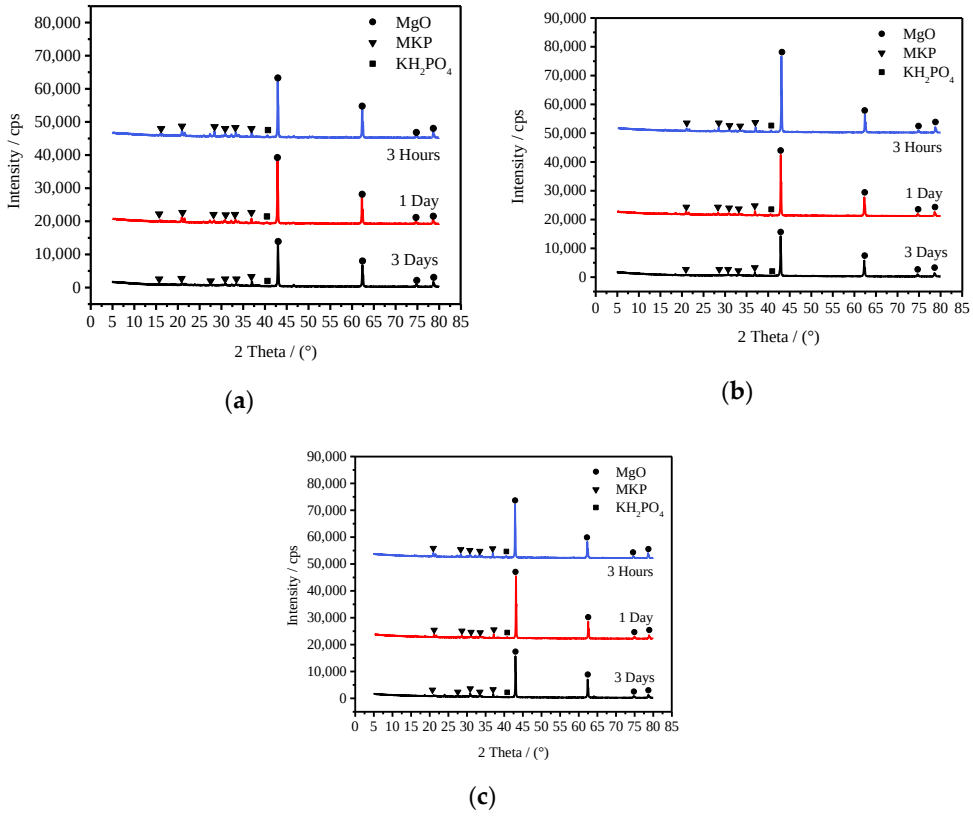

Figure 9. X-ray diffraction patterns of specimens. (**a**) Specimens with 0% MgCl, (**b**) Specimens with 2% MgCl, (**c**) Specimens with 4% MgCl.

Figure 10 shows the scanning electron microscope (SEM) results of specimens. The energy dispersive spectrometer (EDS) is illustrated in Figure 11. Specimen with 4% MgCl and cured for 28 days was selected for the investigation of EDS. Table 4 is the element

distribution obtained by EDS. As observed from Figures 10 and 11, rhombic crystal products, which are the early hydration products, can be found in Figure 10. Moreover, with the addition of magnesium chloride, the rhombic crystal products decreased, and the magnesium chloride crystals increased. The increasing curing age improved the density of microstructure and reduced the rhombic crystal products. Moreover, some cracks can be found in the SEM images due to the hydration heat and shrinkage. Furthermore, the addition of magnesium chloride could reduce crack width and the number of inner specimens. It could be summarized from the SEM results that the magnesium chloride could inhibit hydration of magnesium phosphate cement when the curing age was 3 h. Additionally, the inner cracks of magnesium phosphate cement paste were decreased by adding the magnesium chloride.

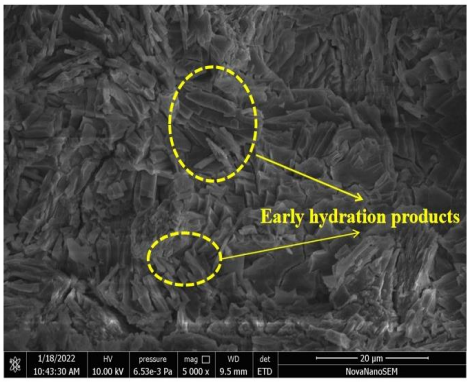

(**a**)

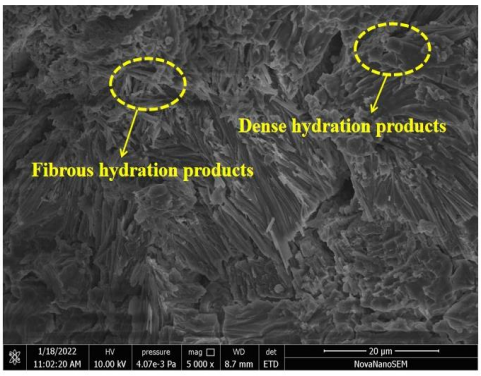

(**b**)

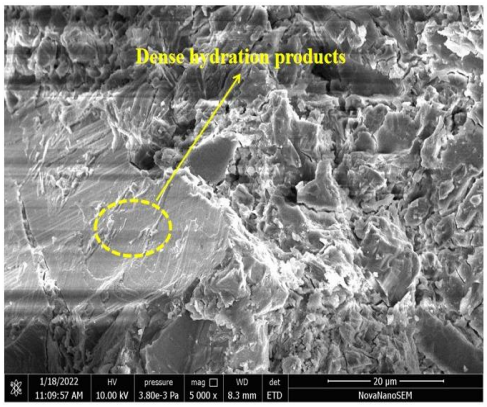

(**c**)

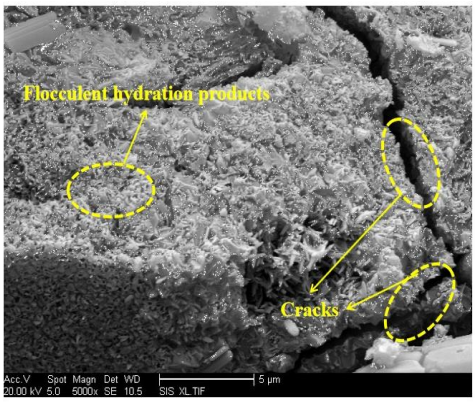

(**d**)

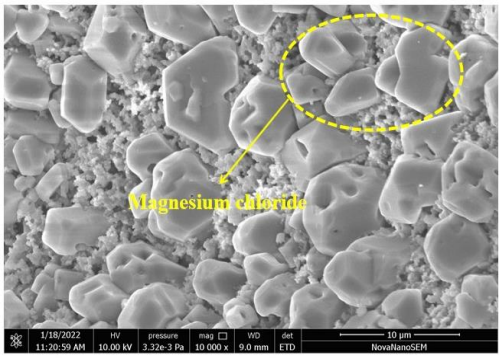

(**e**)

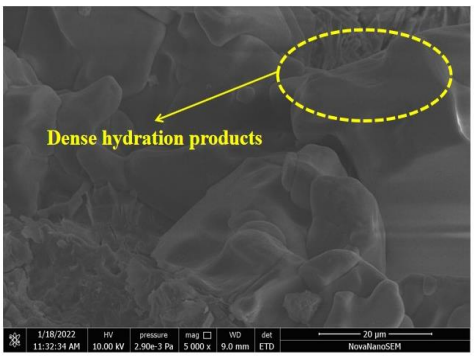

(**f**)

Figure 10. *Cont.*

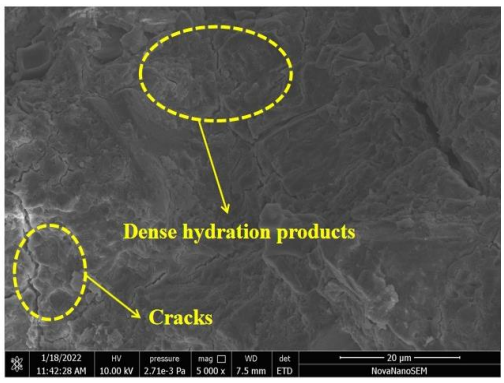

(**g**)

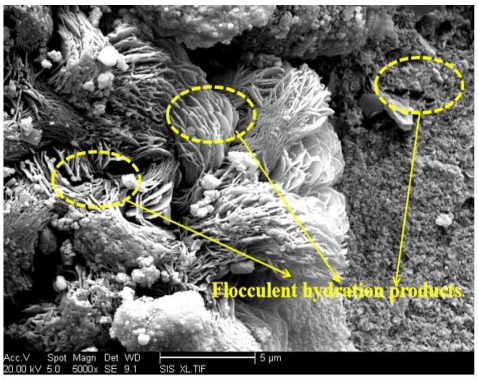

(**h**)

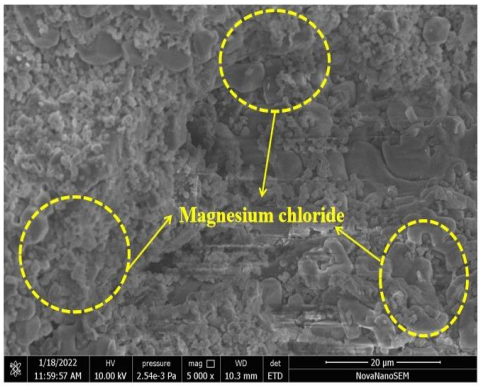

(**i**)

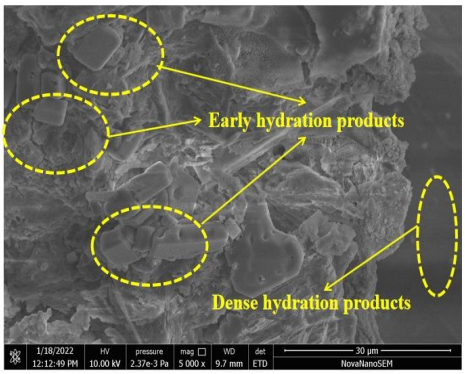

(**j**)

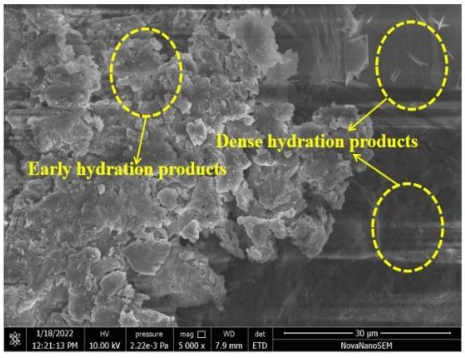

(**k**)

(**l**)

Figure 10. SEM micrographs of specimens. (**a**) Cured for 3 h-0% MgCl, (**b**) Cured for 1d-0% MgCl, (**c**) Cured for 3 d-0% MgCl, (**d**) Cured for 28 d-0% MgCl, (**e**) Cured for 3 h-2% MgCl, (**f**) Cured for 1 d-2% MgCl, (**g**) Cured for 3 d-2% MgCl, (**h**) Cured for 28 d-2% MgCl, (**i**) Cured for 3 h-4% MgCl, (**j**) Cured for 1 d-4% MgCl, (**k**) Cured for 3 d-4% MgCl, (**l**) Cured for 28 d-4% MgCl.

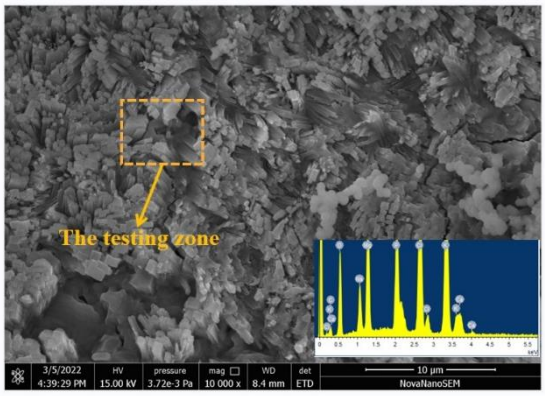

Figure 11. EDS of samples with 4% MgCl cured for 28 days.

Table 4. The element distribution obtained by EDS.

Sample	C	O	Na	Mg	P	Cl	K	Ca
With 4% MgCl	8.29	27.48	3.59	8.66	8.32	18.26	22.14	3.26

4. Conclusions

In this study, the influence of magnesium chloride on the working performance and the mechanical properties of phosphate cement paste was investigated. The microscopic analysis was carried out to investigate the mechanism of the macroscopic properties. The conclusions can be drawn as follows:

The addition of magnesium chloride increased the setting time and the slump flow of phosphate cement paste. The optimal content of 2% magnesium chloride by the mass ratio of magnesium oxide showed the most effective retarding efficiency for phosphate cement paste. The initial and final setting times of 33.5 $\pm$ 0.018 min and 56.8 $\pm$ 0.016 min were observed, respectively. The relationship between the slump flow and the magnesium chloride content obeyed the positively correlated linear function.

The evaluation function for the drying shrinkage rate and the curing age could be expressed as a quadratic function. The addition of magnesium chloride negatively affected the mechanical strengths of phosphate cement pastes at a curing age lower than or equal to 3 d. Meanwhile, when the curing age was longer than 3 d, the addition of magnesium chloride improved the mechanical strengths of phosphate cement paste. Additionally, magnesium chloride decreased the drying shrinkage rate of phosphate cement paste.

The TG test showed that the free water in phosphate cement paste evaporated within temperatures from 20 °C to 150 °C. The decomposition of hydrated potassium magnesium concentrated on two temperature ranges: 150 °C~424 °C and 424 °C~918 °C. The magnesium chloride inhibited the hydration of phosphate cement and reduced cracks induced by drying shrinkage at a later curing age (higher than 3 d). The retarder composed of magnesium chloride and borax showed a positive effect on retarding phosphate cement setting and improved its properties at a curing age longer than 3 d.

Author Contributions: Conceptualization, Y.D. and H.W.; methodology, Y.D. and P.G.; software, S.Z. and T.D.; validation, Y.D., J.Y. and T.D.; formal analysis, Y.D.; investigation, Y.D.; resources, H.W. and Z.W.; data curation, Y.D. and T.D.; writing—original draft preparation, Y.D.; writing—review and editing, H.W. and Y.D.; visualization, Z.W.; supervision, P.G.; project administration, Y.D. and H.W.; funding acquisition, Y.D. All authors have read and agreed to the published version of the manuscript.

Funding: This work was sponsored by the National Nature Science Foundation of China (NSFC) (Grant No. 51578475), Jiangsu Science and Technology Department (Industry-university-research cooperation project 2020. No. BY2020359), Zhejiang Provincial Natural Science Foundation [No. Y22E081344], the National Natural Science Foundation of China [No. 51808300], the Natural Science Foundation of Jiangsu Province (No. BK20200655), the Shuangchuang Program of Jiangsu Province (No. JSSCBS20211195), and Jiangxi Province traffic construction Program (No. 2020H0047).

Institutional Review Board Statement: Not applicable.

Informed Consent Statement: Not applicable.

Data Availability Statement: The data used to support the findings of this study are available from the corresponding author upon request.

Conflicts of Interest: The authors declare that there are no conflict of interest regarding the publication of this paper.

References

1. Li, Y.; Li, X.; Tan, Y. Effect of aging on fatigue performance of cement emulsified asphalt repair material. *Constr. Build. Mater.* **2021**, *292*, 123417. [CrossRef]
2. Wei, Y.; Gao, X.; Zhang, Q. Evaluating performance of concrete pavement joint repair using different materials to reduce reflective cracking in asphalt concrete overlay. *Road Mater. Pavement Des.* **2014**, *15*, 966–976. [CrossRef]
3. Qiao, F.; Chau, C.; Li, Z. Property evaluation of magnesium phosphate cement mortar as patch repair material. *Constr. Build. Mater.* **2010**, *24*, 695–700. [CrossRef]
4. Huang, G.; Wang, H.; Shi, F. Coupling Effect of Salt Freeze-thaw Cycles and Carbonation on the Mechanical Performance of Quick Hardening Sulphoalu-minate Cement-based Reactive Powder Concrete with Basalt Fibers. *Coatings* **2021**, *11*, 1142. [CrossRef]
5. Wang, Y.; Ye, J.; Liu, Y.; Qiang, X.; Feng, L. Influence of freeze–thaw cycles on properties of asphalt-modified epoxy repair materials. *Constr. Build. Mater.* **2013**, *41*, 580–585. [CrossRef]
6. Ahmad, M.; Chen, B.; Haque, M. Multiproperty characterization of cleaner and energy-efficient vegetal concrete based on one-part geopolymer binder. *J. Clean. Prod.* **2020**, *253*, 119916. [CrossRef]
7. Hong, X.; Wang, H.; Shi, F. Influence of NaCl freeze thaw cycles and cyclic loading on the mechanical performance and permeability of sulphoaluminate cement reactive powder concrete. *Coatings* **2020**, *10*, 1227. [CrossRef]
8. Zhang, C.; Wang, H. Influence of NaCl Freeze–thaw Cycles on the Mechanical Strength of Reactive Powder Concrete with the Assembly Unit of Sulphoaluminate Cement and Ordinary Portland Cement. *Coatings* **2021**, *11*, 1238.
9. Singh, M.; Kapur, P.; Pradip. Preparation of calcium sulphoaluminate cement using fertiliser plant wastes. *J. Hazard. Mater.* **2008**, *157*, 106–113. [CrossRef] [PubMed]
10. Cai, G.; Zhao, J. Application of sulphoaluminate cement to repair deteriorated concrete members in chloride ion rich environment-A basic experimental investigation of durability properties. *KSCE J. Civil Eng.* **2016**, *20*, 2832–2841. [CrossRef]
11. Xu, L.; Liu, S.; Li, N.; Peng, Y.; Wu, K.; Wang, P. Retardation effect of elevated temperature on the setting of calcium sulfoaluminate cement clinker. *Constr. Build. Mater.* **2018**, *178*, 112–119. [CrossRef]
12. Mestres, G.; Aguilera, F.S.; Manzanares, N.; Sauro, S.; Osorio, R.; Toledano, M.; Ginebra, M.P. Magnesium phosphate cements for endodontic applications with improved long-term sealing ability. *Int. Endod. J.* **2014**, *47*, 127–139. [CrossRef]
13. Ding, Z.; Dong, B.; Xing, F.; Han, N.; Li, Z. Cementing mechanism of potassium phosphate based magnesium phosphate cement. *Ceram. Int.* **2012**, *38*, 6281–6288. [CrossRef]
14. Xu, B.; Ma, H.; Li, Z. Influence of magnesia-to-phosphate molar ratio on microstructures, mechanical properties and thermal conductivity of magnesium potassium phosphate cement paste with large water-to-solid ratio. *Cem. Concr. Res.* **2015**, *68*, 1–9. [CrossRef]
15. Li, Y.; Sun, J.; Chen, B. Experimental study of magnesia and M/P ratio influencing properties of magnesium phosphate cement. *Constr. Build. Mater.* **2014**, *65*, 177–183. [CrossRef]
16. Ostrowski, N.; Roy, A.; Kumta, P.N. Magnesium phosphate cement systems for hard tissue applications: A review. *ACS Biomater. Sci. Eng.* **2016**, *2*, 1067–1083. [CrossRef] [PubMed]
17. Du, Y.; Gao, P.; Yang, J.; Shi, F. Research on the Chloride Ion Penetration Resistance of Magnesium Phosphate Cement (MPC) Material as Coating for Reinforced Concrete Structures. *Coatings* **2020**, *10*, 1145. [CrossRef]
18. Li, Y.; Chen, B. Factors that affect the properties of magnesium phosphate cement. *Constr. Build. Mater.* **2013**, *47*, 977–983. [CrossRef]
19. Chau, C.K.; Fei, Q.; Li, Z. Microstructure of magnesium potassium phosphate cement. *Constr. Build. Mater.* **2011**, *25*, 2911–2917. [CrossRef]
20. Yang, Q.; Zhu, B.; Wu, X. Characteristics and durability test of magnesium phosphate cement-based material for rapid repair of concrete. *Mater. Struct.* **2000**, *33*, 229–234. [CrossRef]
21. Pera, J.; Ambroise, J. Fiber-reinforced Magnesia-phosphate Cement Composites for Rapid Repair. *Cem. Concr. Compos.* **1998**, *20*, 31–39. [CrossRef]

22. Fang, Y.; Chen, B.; Oderji, S.Y. Experimental research on magnesium phosphate cement mortar reinforced by glass fiber. *Constr. Build. Mater.* **2018**, *188*, 729–736. [CrossRef]
23. Qin, J.; Qian, J.; Li, Z.; You, C.; Dai, X.; Yue, Y.; Fan, Y. Mechanical properties of basalt fiber reinforced magnesium phosphate cement composites. *Constr. Build. Mater.* **2018**, *188*, 946–955. [CrossRef]
24. Tang, H.; Qian, J.; Ji, Z.; Dai, X.; Li, Z. The protective effect of magnesium phosphate cement on steel corrosion. *Constr. Build. Mater.* **2020**, *255*, 119422. [CrossRef]
25. Yaphary, Y.; Yu, Z.; Lam, R.; Lau, D. Effect of triethanolamine on cement hydration toward initial setting time. *Constr. Build. Mater.* **2017**, *141*, 94–103. [CrossRef]
26. *GB/T 1346-2011*; Test Methods for Water Requirement of Normal Consistency, Setting Time and Soundness of the Portland Cement. The State Bureau of Quality and Technical Supervision: Beijing, China, 2011.
27. *GB/T 17671-1999*; Method of Testing Cements—Determination of Strength. The State Bureau of Quality and Technical Supervision: Beijing, China, 1999.
28. Yang, J.; Huang, J.; Su, Y.; He, X.; Tan, H.; Yang, W.; Strnadel, B. Eco-friendly treatment of low-calcium coal fly ash for high pozzolanic reactivity: A step towards waste utilization in sustainable building material. *J. Clean. Prod.* **2019**, *238*, 117962. [CrossRef]
29. Wang, H.; Hu, L.; Cao, P.; Luo, B.; Tang, J.; Shi, F.; Yu, J.; Li, H.; Jin, K. The Application of Electrical Parameters to Reflect the Hydration Process of Cement Paste with Rice Husk Ash. *Materials* **2019**, *12*, 2815. [CrossRef] [PubMed]
30. Wang, H.; Zhang, A.; Zhang, L.; Wang, Q.; Han, Y.; Liu, J.; Gao, X.; Shi, F.; Lin, X.; Feng, L. Hydration process of rice husk ash cement paste and the following corrosion resistance of embedded steel bar. *J. Cent. South Univ.* **2020**, *11*, 3464–3476. [CrossRef]
31. Seehra, S.; Gupta, S.; Kumar, S. Rapid setting magnesium phosphate cement for quick repair of concrete pavements-characterisation and durability aspects. *Cem. Concr. Res.* **1993**, *23*, 254–266. [CrossRef]
32. Yang, J.; Shi, C.; Chang, Y.; Yang, N. Hydration and hardening characteristics of magnesium potassium phosphate cement paste containing composite retarders. *J. Build. Mater.* **2013**, *16*, 43–48.
33. Yang, Q.; Zhu, B.; Zhang, S.; Wu, X. Properties and applications of magnesia–phosphate cement mortar for rapid repair of concrete. *Cem. Concr. Res.* **2000**, *30*, 1807–1813. [CrossRef]
34. You, C.; Qian, J.; Qin, J.; Wang, H.; Wang, Q.; Ye, Z. Effect of early hydration temperature on hydration product and strength development of magnesium phosphate cement (MPC). *Cem. Concr. Res.* **2015**, *78*, 179–189. [CrossRef]
35. Viani, A.; Gualtieri, A. Preparation of magnesium phosphate cement by recycling the product of thermal transformation of asbestos containing wastes. *Cem. Concr. Res.* **2014**, *58*, 56–66. [CrossRef]
36. Dong, J.; Yu, H.; Zhang, L. Study on experimental conditions of hydration methods of determining active magnesium oxide content. *Salt Lake Res.* **2010**, *18*, 38–41.
37. Walling, S.; Provis, J. Magnesia-based cements: A journey of 150 years, and cements for the future? *Chem. Rev.* **2016**, *116*, 4170–4204. [CrossRef]
38. Yang, J.; Li, T.; Xu, X. Effect of Fine Aggregates on Properties of Magnesium Potassium Phosphate Cement Mortar. *J. Mater. Civ. Eng.* **2017**, *29*, 06017012.
39. Li, Y.; Shi, T.; Li, Y.; Bai, W.; Lin, H. Damage of magnesium potassium phosphate cement under dry and wet cycles and sulfate attack. *Constr. Build. Mater.* **2019**, *210*, 111–117. [CrossRef]
40. Wu, C.; Yu, H. Preparation and properties of modified magnesium oxysulfate cement derived from waste sulfuric acid. *Adv. Cem. Res.* **2016**, *28*, 178–188.
41. Nergis, D.D.B.; Vizureanu, P.; Sandu, A.; Nergis, D.P.B.; Bejinariu, C. XRD and TG-DTA Study of New Phosphate-Based Geopolymers with Coal Ash or Metakaolin as Aluminosilicate Source and Mine Tailings Addition. *Materials* **2022**, *15*, 202. [CrossRef]